Title: Magnetization processes of fractal-like core shell nanoparticles

Author: Grzegorz Ziółkowski, Artur Chrobak, Dariusz Chrobak

Citation style: Ziółkowski Grzegorz, Chrobak Artur, Chrobak Dariusz. (2021). Magnetization processes of fractal-like core shell nanoparticles. "Journal of Magnetism and Magnetic Materials " (2021), Vol. 0, art. no. 168800, s. 1-6. DOI: 10.1016/j.jmmm.2021.168800

Journal of Magnetism and Magnetic Materials xxx (xxxx) xxx

Contents lists available at ScienceDirect

Journal of Magnetism and Magnetic Materials

journal homepage: www.elsevier.com/locate/jmmm

Magnetization processes of fractal-like core shell nanoparticles

Grzegorz Ziółkowski [a,*], Artur Chrobak [a], Dariusz Chrobak [b]

[a] Institute of Physics, University of Silesia in Katowice, 75 Pułku Piechoty 1A, 41-500 Chorzów, Poland
[b] Institute of Materials Engineering, University of Silesia in Katowice, 75 Pułku Piechoty 1A, 41-500 Chorzów, Poland

ARTICLE INFO

Keywords:
Monte Carlo simulations
Hard magnetic properties
Diffusion Limited Aggregation

ABSTRACT

The paper refers to micromagnetic simulations of magnetization processes of fractal-like core–shell nanoparticles. The objects were generated using the 3D diffusion limited aggregation (DLA) algorithm for obtaining fractals with two kinds of magnetic phases – magnetically soft core and magnetically hard shell. The simulations were carried out using the cluster Monte Carlo algorithm designed for spin continuous and multiphase magnetic systems. The presented research includes different degrees of branch development, different strengths of the exchange coupling between the phases, as well as different soft phase contents. As was shown, the influence of microstructure on the coercivity mechanism is a complex phenomenon. The core–shell coupling and the magnetic properties of the entire system can be controlled by fractal development. The spring-exchange mechanism and high surface development of the fractals makes it possible to obtain a value of the $|BH|_{max}$ parameter higher than 300 kJ/m^3. For $K = 5 \times 10^{-5}$ eV and $K = 5 \times 10^{-4}$ eV, it requires about 30% and 7% contribution of the hard magnetic phase, respectively.

1. Introduction

Magnetic materials are very important in current technologies [1–7]. New and continuously increasing requirements can be fulfilled by modern nanostructured magnetic composites containing phases characterized by different magnetic properties. Recently, we reported ultra-high coercivity (>7 T) in Fe-Nb-B-Tb type of bulk nanocrystalline alloys prepared by the vacuum suction technique [8,9]. It was shown that in such materials the interactions between relatively soft ($TbFe_2$) and hard magnetic phases ($Tb_2Fe_{14}B$) with specific irregular branches are especially important and can lead to the emergence of new and unique properties. On the other hand, the antiferromagnetic coupling between Fe and Tb limits the maximum of magnetic saturation and, as a consequence, reduces the application potential for such materials.

However, the grains with ultra-high coercivity may be a key element for the composites also containing some soft magnetic phases (like Fe), and via the interactions with their surroundings can lead to improved magnetic remanence of the composite. Therefore, a better understanding of the interactions in such systems, including the optimal balance between soft and hard phases as well as impact of system geometry on macroscopic properties, is essential.

An obvious geometric configuration is a spherical core–shell system. Magnetic coupling between the core and shell depends on exchange energy, which is related to exchange interactions as well as a number of interacting magnetic moments. The latter factor is directly attributed to the geometry of the system and, for the spherical one, is defined by the diameter of the core and density of the material. A decrease in the diameter leads to a decrease in the interface surface, consequently weakening the core–shell coupling.

In order to enhance the interface coupling, we propose designing the core as a fractal-like object. Theoretically, it is possible to generate such a shape with a ratio of spins on the surface to spins in the volume higher than for pure spherical configuration. In this way, the decreasing mean diameter of the particle may keep the core–shell coupling relatively strong. Practically, fractal-like objects can be found in early stages of crystallization (dendrite grains) as well as in layer growth during chemical or molecular beam deposition.

In this work, we present the magnetic properties of fractal-like core–shell systems studied using Monte Carlo magnetic simulations. The geometry of the systems was generated using the Diffusion Limited Aggregation (DLA) algorithm, allowing us to obtain cores with different developments of their surface. The main goal of this study is to present the possibility of creating and enhancing hard magnetic properties in the particles with a soft magnetic core and hard magnetic shell.

* Corresponding author.
E-mail address: grzegorz.ziolkowski@us.edu.pl (G. Ziółkowski).

https://doi.org/10.1016/j.jmmm.2021.168800
Received 11 July 2021; Received in revised form 17 October 2021; Accepted 21 October 2021
Available online 12 November 2021

Table 1
The main simulation parameters.

Parameter	Value
System size	40 × 40 × 40 nodes (11.2 nm × 11.2 nm × 11.2 nm)
Distance between nodes	0.28 nm
Dipolar constant	2.15×10^{-7} eV nm^3
Anisotropy constant (core)	0 eV
Anisotropy constant (shell)	5×10^{-5} eV, 5×10^{-4} eV
Spin (core)	1
Spin (shell)	0.6, 0.2
Exchange integral parameter (core and shell), J	1.5×10^{-2} eV
Annealing temperature k_BT	10^{-5} eV
DLA adding probability	100%, 10%, 1%, 0.1%, 0.01%
Number of core particles, N_{Core}	7000
Number of shell particles, N_{Shell}	500, 2000, 5000
Contribution of core surface to the all core particles $N_S/(N_S \pm N_V)$	0.3, 0.5, 0.7

2. Simulation procedure and simulated systems

In the presented work, we performed a series of magnetization process simulations for several fractal-like core–shell nanoparticles. The simulations were carried out using the 3D cluster Monte Carlo plus simulated annealing algorithm designed for spin continuous and multiphase magnetic systems (for method description see [10–15]). The objects were generated by the 3D Diffusion Limited Aggregation algorithm that enables fractal-like structures with two kinds of magnetic phases to be obtained – magnetically soft core and magnetically hard shell. The principle of the DLA method consists of 4 main steps (for

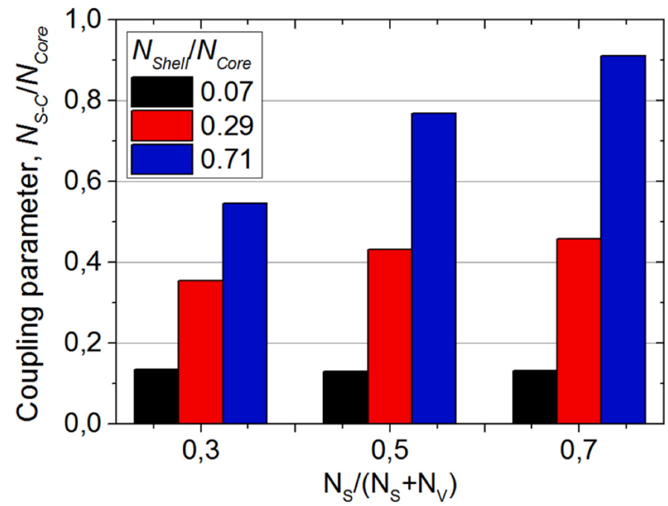

Fig. 2. Influence of fractal core development $N_S/(N_S \pm N_V)$, as well as the shell to the core contribution N_{Shell}/N_{Core} on the coupling parameter between the core and shell $N_{S\text{-}C}/N_{Core}$ (i.e., ratio between number of neighboring spins and number of spins in the core).

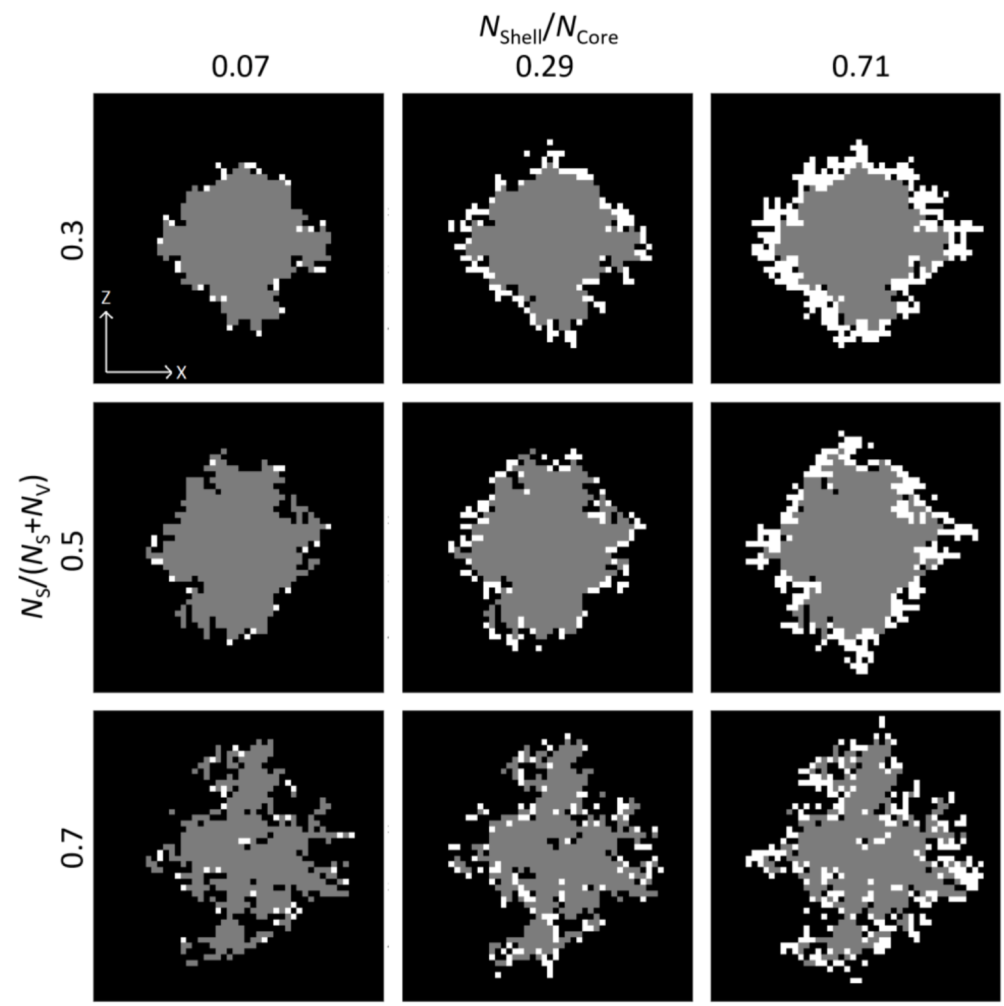

Fig. 1. Central cross section (Y = 20 nodes) of a fractal-like core–shell nanoparticle for different $N_S/(N_S + N_V)$ and DLA adding probability equal to 1%. The gray, white and black colors correspond to the soft (core), hard (shell) and non-magnetic phase, respectively.

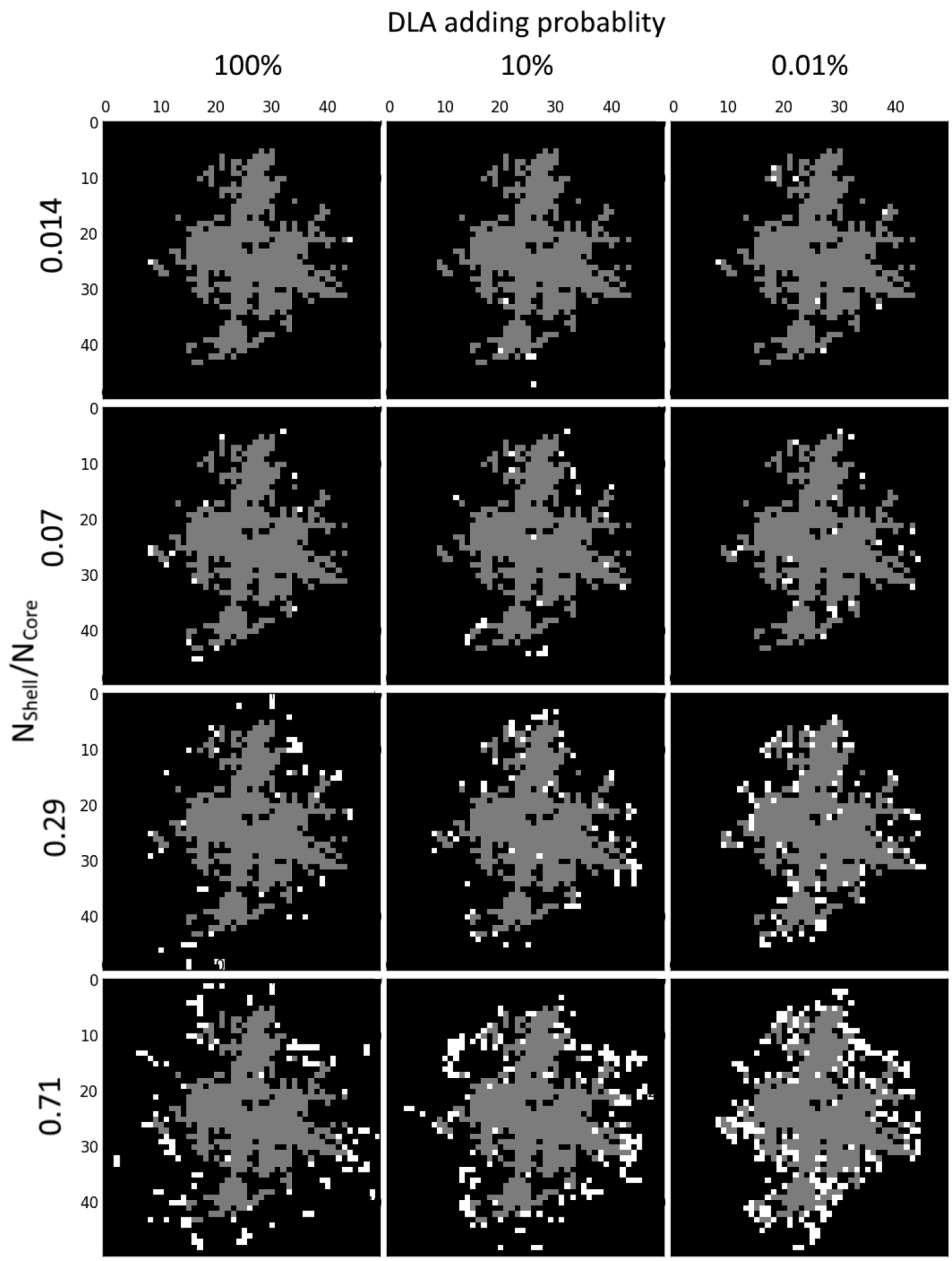

Fig. 3. Cross section of a fractal-like core–shell nanoparticle generated by different DLA adding probability for $N_S/(N_S \pm N_V) = 0.7$. The gray, white and black colors correspond to the soft (core), hard (shell) and non-magnetic phase, respectively.

details see [16–20]):

Place one fixed node in the center of the system and sign it as a fixed scrap of the final particle.
Provide a new scrap to the system starting from its edge. This scrap can move randomly on the nodes until it collides with a fixed one.
In case of collision, the moving scrap will be fixed with the probability called DLA adding probability, and then go to step 2.
In order to obtain multiphase core–shell systems, step 2 is repeated for a given number of core nodes N_{Core}, and then for a given number of shell nodes N_{Shell} with different magnetic properties.

Additionally, the classic DLA method was extended using the internal growth procedure corresponding to the real crystal grain growth phase. The whole system is made up of 40x40x40 nodes with irregular core–shell particles inside (in the center), generated according to the procedure described above using one of the factor sets (see Table 1). Finally, all the generated systems are characterized by four specific parameters: a) the development of core fractal, i.e., a contribution of core surface to the all core particles $N_S/(N_S \pm N_V)$, b) the shell to the core contribution N_{Shell}/N_{Core}, c) the DLA adding probability for shell particles, which may correspond to the preparation method of real core–shell systems (for example, the Molecular Beam Epitaxy for high probability or chemical methods for lower probability) and d) shell magnetic properties corresponding to the Sm-Co magnets ($S = 0.6$, $K = 5 \times 10^{-5}$ eV, coercive field $\mu_0 H_c \approx 1$ T) as well as Fe-Nb-B-Tb type of bulk nanocrystalline materials ($S = 0.2$, $K = 5 \times 10^{-4}$ eV, $\mu_0 H_c \approx 8$ T). In both cases, a soft magnetic core corresponds to the Iron with $S = 1$ and, for simplicity, $K = 0$ eV. Moreover, an easy magnetization axis of a hard magnetic field coincided with the direction of the external magnetic

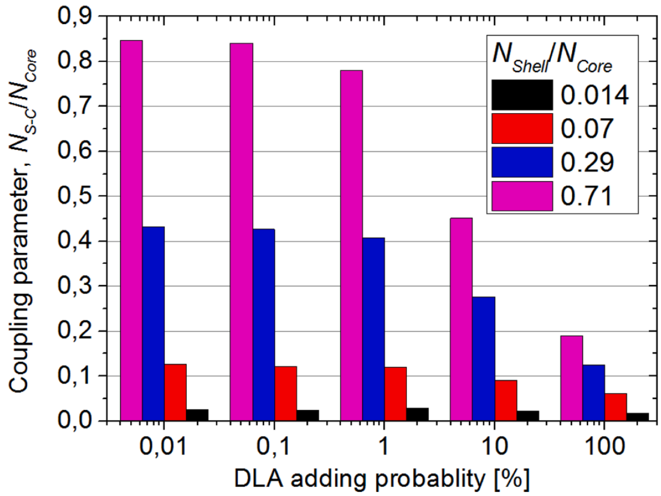

Fig. 4. Influence of DLA adding probability as well as shell to core contribution on the coupling parameter between the core and shell for $N_S/(N_S \pm N_V) = 0.7$.

field, i.e., Z axis. The most important parameters of the simulation procedure are summarized in Table 1.

3. Results and discussion

The cross sections (Y = 20 nodes, i.e., 5.6 nm) for the selected generated systems were presented in Fig. 1. The number of neighboring spins (contacts) between the core and the shell $N_{C\text{-}S}$, is especially important, depending on the development of the core fractal $N_S/(N_S \pm N_V)$, as well as the shell to core contribution N_{Shell}/N_{Core}. The summary of the number of these parameters in relation to all core particles is presented in Fig. 2. It can be seen that the number of contacts, and hence the coupling between the two phases, increases with the increase in the core surface area, as well as the number of shell particles. A significant advantage of the core with a fractal-like geometry and well-developed branches is a very high surface area contribution in relation to the volume. In contrast, for spherical-like particles, the surface to volume ratio decreases sharply as the radius increases and, as a consequence, limits the strength of coupling with the surrounding phase. The systems with the most developed core, i.e., $N_S/(N_S \pm N_V) = 0.7$, were selected for further analysis due to their high potential for strong magnetic coupling between the hard and soft magnetic phase.

Another important parameter influencing the coupling strength is the DLA adding probability. Fig. 3 presents the cross section of selected systems depending on DLA adding probability as well as the N_{shell}/N_{core} parameter. Moreover, the calculated $N_{S\text{-}C}/N_{Core}$ values were presented in Fig. 4. It can be seen that the coupling greatly increases from 0.19 to 0.78 with the decrease in the DLA adding probability from 100% to 1%, respectively. On the other hand, further reducing the probability does not lead to such dramatic changes, as the maximum equals about 0.85 when the DLA adding probability is 0.01%. This observation may be particularly important from the preparation method point of view of the real core–shell systems. Due to the irregular branches present on the core surface, the shell particles sprayed from outside the system with 100% adding probability have a very little chance to penetrate into the core structure and cover the entire available surface of the branches.

A greater number of contacts between the core and the shell can lead to a stronger magnetic coupling between these phases, and thus may influence the magnetic behavior of the entire system. This trend can be observed in the reverse magnetization curves presented in Fig. 5. For a better analysis, the coercive field H_C as well as the maximum energy product $|BH|_{max}$, estimated for all simulated curves are summarized in Fig. 6. It may be noted that the coercivity increases with the increase in the shell contribution and its anisotropy, as well as with the decrease in DLA adding probability. For example, in the case of $N_{Shell}/N_{Core} = 0.29$ where shell anisotropy equals 5×10^{-4} eV, the coercive field increases from 1.1 T to 1.6 T for the DLA adding probability equal to 100% and 0.01%, respectively, which means an increase of 45%. A similar situation can also be observed for the lower shell anisotropy (5×10^{-5} eV),

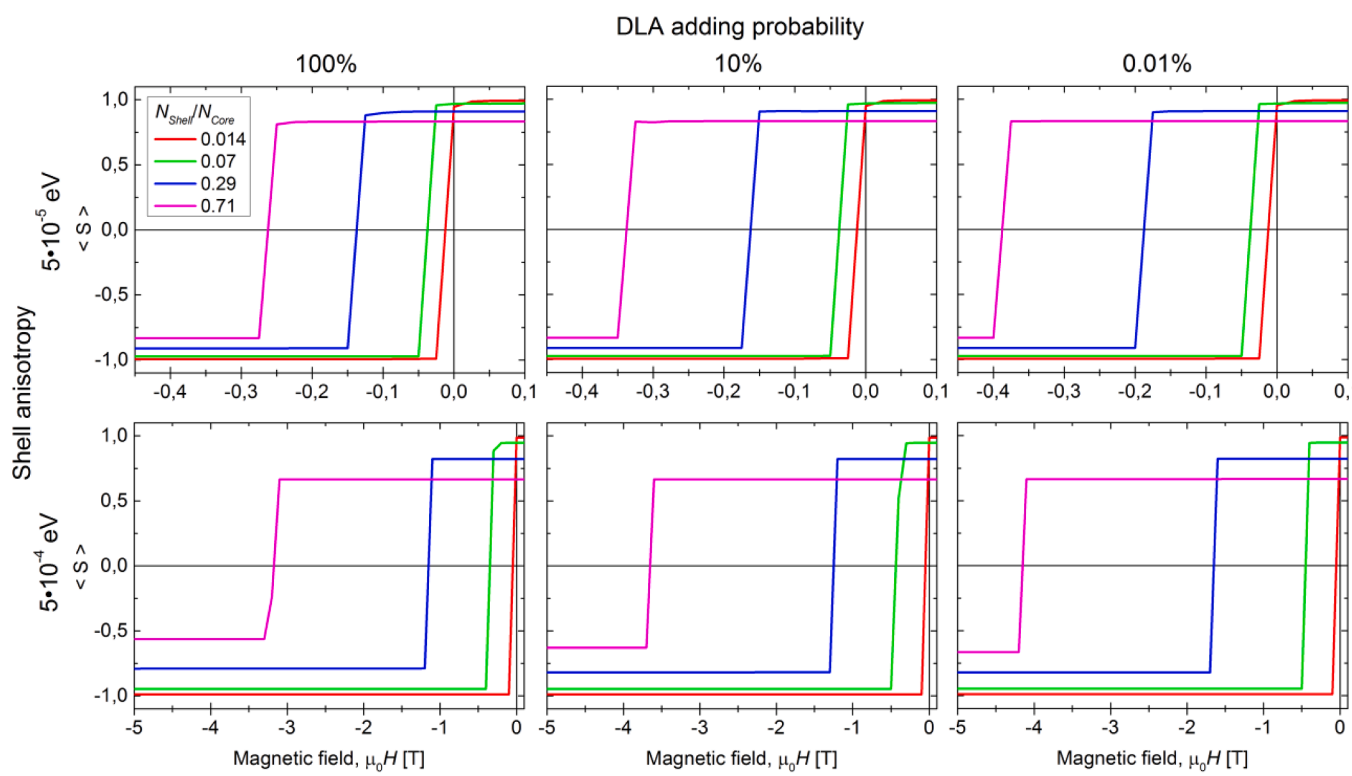

Fig. 5. Simulated reverse magnetization curves for all studied cases.

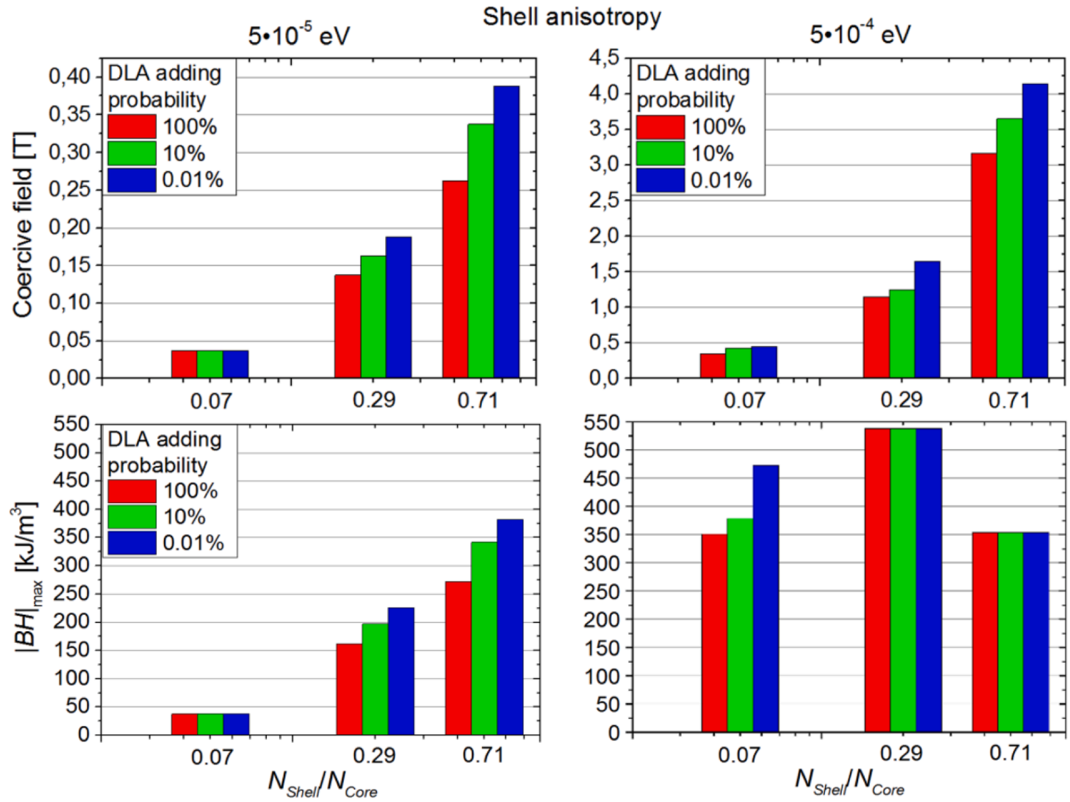

Fig. 6. Coercive field and estimated $|BH|_{max}$ parameter for all studied cases.

for example, H_C increases by 50% from 0.26 T up to 0.39 T when $N_{Shell}/N_{Core} = 0.71$. Moreover, the increase in the coercive field entails, in some cases, an increase in the maximum energy product. Based on the simulations carried out, one may note that a $|BH|_{max}$ parameter higher than 220 kJ/m^3 when $N_{Shell}/N_{Core} = 0.29$ and shell anisotropy equals 5×10^{-5} eV or even higher than 470 kJ/m^3 using just 7% contribution of the hard magnetic phase with anisotropy equals 5×10^{-4} eV.

Taking into account the results of the performed simulations, it can be seen that increasing the development of the core surface can improve the hard magnetic properties of the entire material, even with a relatively small amount of hard phase. The obtained values of the maximum energy product close to 200–300 kJ/m^3 have a high application potential and can fill the gap between conventional and neodymium magnets. By using the shell with coercivity of about 1 T (i.e. $K = 5 \times 10^{-5}$eV), these values can be obtained from about 30% of the hard magnetic phase, while in the case of a shell with ultra-high coercivity ($K = 5 \times 10^{-4}$ eV), even less than 10% of the hard magnetic phase is sufficient. It is important to remember that the simulations assume the most advantageous variant from the hard magnetic properties point of view, i.e., the easy magnetization axis of the hard phase coincides with the direction of the external magnetic field. In the real materials, these directions may differ from each other; therefore, lower values of $|BH|_{max}$ are expected. Nevertheless, the obtained results demonstrate the potential of this approach in the design of new hard magnetic materials with a reduced content of rare earths.

4. Conclusions

The main results can be summarized as follows:

- The core–shell coupling parameter strongly depends on the fractal surface development and the DLA adding probability. The most effective coupling between the core and shell was obtained for the fractals with $N_S/(N_S + N_V) = 0.7$ and DLA adding probability $\leq 1\%$.
- The used MC algorithm facilitated the simulation of reverse magnetization curves and determination of the anisotropy field of the studied fractals.
- As shown, the anisotropy fields strongly depend on the N_{Shell}/N_{Core} ratio and magnetic anisotropy attributed to the shell.
- Increase in the shell contribution as well as the coupling parameter result in the observed gradual increase in the anisotropy fields.
- The spring-exchange mechanism and high surface development of the fractal make it possible to obtain a value of the $|BH|_{max}$ parameter higher than 300 kJ/m^3. For $K = 5 \times 10^{-5}$ eV and $K = 5 \times 10^{-4}$ eV, it requires about 30% and 7% contribution of the hard magnetic phase, respectively.

Declaration of Competing Interest

The authors declare that they have no known competing financial interests or personal relationships that could have appeared to influence the work reported in this paper.

Acknowledgments

This work was supported by National Science Center in Poland with the grant 2015/19/B/ST8/02636.

References

[1] K.H.J. Buschow, F.R. de Boer (Eds.), Physics of Magnetism and Magnetic Materials, Springer US, Boston, MA, 2003.
[2] J.M.D. Coey, Magnetism and Magnetic Materials, Cambridge University Press, 2010.
[3] F.E. Luborsky, Permanent magnets in use today, J. Appl. Phys. 37 (1966) 1091–1094.
[4] M. Sagawa, S. Fujimura, H. Yamamoto, Y. Matsuura, K. Hiraga, Permanent magnet materials based on the rare earth-iron-boron tetragonal compounds, IEEE Trans. Magn. 20 (1984) 1584–1589.

[5] O. Gutfleisch, Controlling the properties of high energy density permanent magnetic materials by different processing routes, J. Phys. D: Appl. Phys. 33 (2000) 157–172.

[6] A.S. Rao, Alnico permanent magnets an overview, Proceedings of Electrical/ Electronics Insulation Conference (1993) 373–383.

[7] J.J. Croat, J.F. Herbst, R.W. Lee, F.E. Pinkerton, Pr Fe and Nd Fe based materials: a new class of high performance permanent magnets, J. Appl. Phys. 55 (1984) 2078–2081.

[8] A. Chrobak, G. Ziółkowski, N. Randrianantoandro, Magnetic hardening of Fe–Nb–B–Tb type of bulk nanocrystalline alloys, J. Alloys Compd. 583 (2014) 48–54.

[9] A. Chrobak, G. Ziółkowski, N. Randrianantoandro, J. Klimontko, D. Chrobak, K. Prusik, Ultra-high coercivity of $(Fe_{86-x}Nb_xB_{14})_{0.88}Tb_{0.12}$ bulk nanocrystalline magnets, J. Rak Acta Mater. 98 (2015) 318–326.

[10] A. Chrobak, G. Ziółkowski, K. Granek, D. Chrobak, Disorder-based cluster Monte Carlo algorithm and its application in simulations of magnetization processes, Comput. Phys. Commun. 238 (2019) 157–164.

[11] A. Chrobak, G. Ziółkowski, D. Chrobak, G. Chełkowska, From atomic level to large-scale Monte Carlo magnetic simulations, Materials 13 (2020) 1–11.

[12] D.P. Landau, K. Binder (Eds.), A Guide to Monte Carlo Simulations in Statistical Physics, Cambridge University Press, Cambridge, 2014.

[13] D. Vanderbilt, S.G. Louie, A Monte Carlo simulated annealing approach to optimization over continuous variables, J. Comput. Phys. 56 (1984) 259–271.

[14] A. Chrobak, G. Haneczok, G. Chełkowska, A. Kassiba, G. Ziółkowski, Numerical analysis of superparamagnetic clusters distribution, Phys. Status Solidi A 208 (2011) 2692–2698.

[15] V. Fabian, Simulated annealing simulated, Comput. Math. Appl. 33 (1997) 81–94.

[16] T.A. Witten, L.M. Sander, Diffusion-limited aggregation: A kinetic critical phenomenon, Phys. Rev. Lett. 47 (1981) 1400–1403.

[17] L.M. Sander, Fractal growth processes, Nature 322 (1986) 789–793.

[18] T.A. Witten, L.M. Sander, Diffusion-limited aggregation, Phys. Rev. B 27 (1983) 5686.

[19] L.M. Sander, Z.M. Cheng, R. Richter, Diffusion-limited aggregation in three dimensions, Phys. Rev. B 28 (1983) 6394–6396.

[20] P.D. Bourke, Constrained diffusion limited aggregation in 3 dimensions, Comput. Graph. 30 (2006) 646–649.